

Simulation of Anisotropic Etching of Alpha-Quartz for 3D Computer-Aided-Design System

Hisanori Hayashi and Toshitsugu Ueda

Waseda University, Graduate School of Information, Production and Systems,
2-2, Hibikino Wakamatsu-ku Kitakyusyu-shi, Fukuoka 808-0135

(Received October 1, 2004; accepted March 29, 2005)

Key words: quartz, anisotropic etching, 3D CAD

Alpha-quartz anisotropic etching is a powerful tool for micromachining for the fabrication of various devices by photolithography. Therefore, this technique can help sensor engineers to develop computer-aided-design (CAD) systems. In this study, we estimated the etching rates of alpha-quartz wafers for all cut angles on the basis of our experimental data. Then, the configuration of the alpha-quartz wafer faces was predicted with the etching rate profile calculated from the experimental data. These results confirmed that our proposed theory corresponds to the experimental results for etching rates in all directions of alpha-quartz. We believe that the results of these simulations lead to the development of a three-dimensional CAD system for the precision design of complex-shaped objects to be fabricated by anisotropic etching of alpha-quartz.

1. Introduction

Micromachining of alpha-quartz wafers by anisotropic etching is applied to the fabrication of various micromachined devices by photolithography, for example, miniature quartz crystal tuning fork resonators for wristwatches and some measurement sensors. It is important for the precision design of micromachined devices to clarify the anisotropic etching properties of quartz and to determine the exact etching rates of all quartz crystal surfaces in all directions. Cheng *et al.*⁽¹⁾ collected data on etching rates using a single-crystal quartz hemispherical specimen. Ueda *et al.*^(2,3) measured the etching rates of quartz wafers for 21 different angles of cut, and interpolated the results with a spline function in order to determine etching rates of all quartz crystal surfaces.

With these quartz anisotropic features, it is useful to apply computer-aided-design (CAD) systems. In this study, we estimated the etching rates of alpha-quartz wafers for all

*Corresponding author, e-mail address: hhayashi@toki.waseda.jp

cut angles according to the etching rate data obtained from an experiment on the anisotropic etching of single-crystal alpha-quartz wafers for various cut angles. After that, we determined the propriety of applying these data to CAD systems.

2. Previous Study

It is difficult to describe the anisotropic etching of a single crystal in terms of the atomic structure of the crystal surface. This is because the etching rate is determined by not only the structure of the crystal surface but also by various complicated factors such as the surface activation energy, intermediate products, mass transfer, and activation ratio.

On the other hand, in cases in which etching anisotropy has been known, there have been attempts to predict the etching shape of a crystal on the basis of the data of anisotropic etching. The method of obtaining the solution locus of a crystal includes the use of Frank's reluctance plot.⁽⁴⁾ Aside from this, Jaccodine (Wulff) has proposed a method for predicting the final shape of a crystal directly from its etching rates. This method involves predicting the final shape on the basis of the condition that the integral of etch rates for all crystal faces is equal to a minimum and is analogous to a plot relating to surface free energy known as a γ plot.⁽⁵⁾

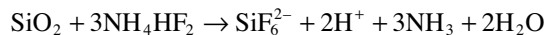
By combining these concepts, we obtained the two conditions that Batterman and Hillocks verified with single-crystal germanium: "a concave face is encircled by faces having a lower etching rate, while a convex face is encircled by faces having a higher etching rate."⁽⁶⁾

If a stripe pattern inactive to an etching solution is formed on a wafer and subsequently etching is carried out, which is one of the objectives of this research, a crystal face having a minimal etching rate within that crystal zone appears inside a hole. In other words, carrying out etching with a stripe pattern formed on a wafer leads to an important conclusion that can be applied to measuring the anisotropic etching rate. That is, it is possible to determine a face having a minimal etching rate within a certain crystal zone.

3. Experiments

3.1 Wafers for experiments

To investigate the etching rates of alpha-quartz wafers in several directions systematically, we performed an experiment on etching of single-crystal alpha-quartz wafers for various cut angles. These were two series of cut angles around the x-axis and y-axis (Fig. 1). The x-axis is vertical to the z-axis and comes out every 120 degrees. The y-axis is vertical to the x-axis and z-axis. The etching solution used in our experiment was ammonium difluoride at 82°C. The reaction of the alpha-quartz and etching solution is as follows.



The z direction of the wafer was used to clarify the direction of minimum etching rate around the x-axis and y-axis. Striped designed mask patterns were formed on the z-wafer along the x-axis and y-axis. Moreover, the directions of minimum etching rate were

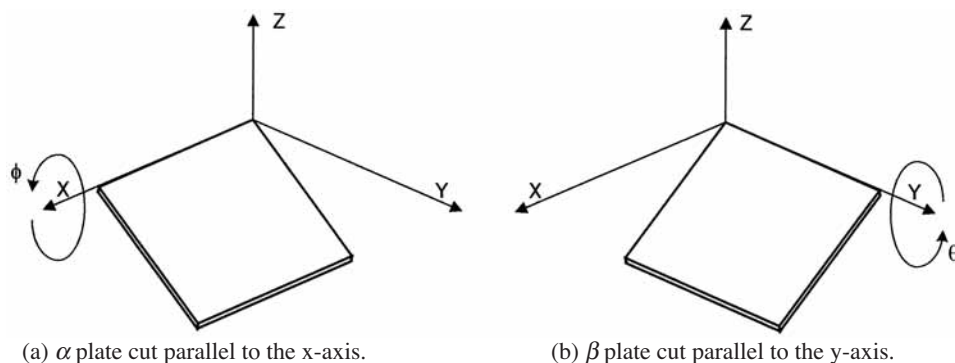


Fig. 1. Orientation of quartz wafers.

obtained for the crystal faces produced by etching a z-directional alpha-quartz wafer plate with an attached striped metal mask under the above-mentioned condition.

Table 1 shows the wafer types of the two series used in the experiment. The reason why the number of wafers cut at the angles formed around the y-axis (rotated x-cut plates) is smaller than the number of wafers cut at the angles formed around the x-axis (rotated y-cut plates) is that the x-axis exhibits twofold symmetry due to the symmetry of the crystal, resulting in the same etching rates being achieved by positive and negative angular rotation of the plate angle. However, for the rotated x-cut plates, the etching rates on either side of a single wafer differ because of the positive and negative values of the x-axis.

3.2 Patterning procedure and equipment

In this section, we detail patterning procedure and experimental equipment. When forming sputtered films on a substrate, particularly one as thin as a quartz wafer, problems can occur such as the deformation of the wafer due to internal stress caused by films or the formation of thin films having significantly different properties on either sides. These problems need to be solved to enable the production of fine metal masks on a quartz wafer and micromachining. Prototyping a double-sided sputtering system and double-sided exposure equipment solved these problems.

In our patterning procedure (Fig. 2), first, chrome and gold metal thin films were deposited on both sides of quartz wafers. Then, photoresist films were deposited on them, and the designed patterns were formed by photolithography. After that, gold and chrome metal films were patterned with a photoresist film as a mask. If electrodes were needed, photoresist films were deposited on the metal film electrode patterns again. Finally, quartz wafers were etched with the metal films as a mask.

In order to realize this procedure, the following equipment was specially designed. Figure 3 shows the double-sided sputtering system. For this system, we redesigned the planetary section of a conventional sputtering system in order to mount rotary wafer holders. As a result of redesigning the wafer holding section to allow the wafer holders to rotate and pass over the target, it is possible to deposit film with the same quality and thickness on each side of a wafer under the same sputtering conditions. The left side of the figure shows a side view of the planetary. This chamber has a motor to rotate the wafer holders and to turn the planetary around. The right side of the figures show a top view of

Table 1

Angles for cutting two series of wafers. (1) “+” corresponds to compression + face. (2) “-” corresponds to compression - face.

Wafer name	Cut angle along y-axis (degree)	Miller index	
$\alpha 1$	75.1	$0\bar{3}\bar{3}1$	
$\alpha 2$	68.9	$0\bar{2}\bar{2}1$	
$\alpha 3$	61.9	$0\bar{3}\bar{3}2$	
$\alpha 4$	51.9	$0\bar{1}\bar{1}1$	
$\alpha 5$	40.5	$0\bar{2}\bar{2}3$	
$\alpha 6$	32.5	$0\bar{1}\bar{1}2$	
$\alpha 7$	22.9	$0\bar{1}\bar{1}3$	
Z	0.0	0001	
$-\alpha 7$	-22.9	$0\bar{1}\bar{1}3$	
$-\alpha 6$	-32.4	$0\bar{1}\bar{1}2$	
$-\alpha 5$	-40.2	$0\bar{2}\bar{2}3$	
$-\alpha 4$	-51.9	$0\bar{1}\bar{1}1$	
$-\alpha 3$	-62.4	$0\bar{3}\bar{3}2$	
$-\alpha 2$	-69.7	$0\bar{2}\bar{2}1$	
$-\alpha 1$	-75.4	$0\bar{3}\bar{3}1$	

Wafer name	Cut angle along y-axis (degree)	Miller index	
		+(1)	-(2)
$\beta 1$	77.2	$4\bar{2}\bar{2}1$	$\bar{4}22\bar{1}$
$\beta 2$	65.6	$2\bar{1}\bar{1}1$	$\bar{2}11\bar{1}$
$\beta 3$	55.7	$4\bar{2}\bar{2}3$	$\bar{4}22\bar{3}$
$\beta 4$	47.7	$2\bar{1}\bar{1}2$	$\bar{2}11\bar{2}$
$\beta 5$	36.3	$2\bar{1}\bar{1}3$	$\bar{2}11\bar{3}$
$\beta 6$	28.8	$2\bar{1}\bar{1}4$	$\bar{2}11\bar{4}$

the chamber and where five holders can be set up. During sputtering these holders rotate inside the chamber and turn around over the wafer target. Thus, metal films are sputtered on both sides of the wafer at the same time. This method prevents the wafer from becoming deformed.

Figure 4 shows the double-sided exposure equipment. In order to carry out etching of the quartz, double-sided exposure equipment is required to form metal masks and electrode patterns on both sides of quartz wafers that have metal thin films sputtered on them. We used Canon's BPA-200 double-sided exposure equipment as the exposure unit because of

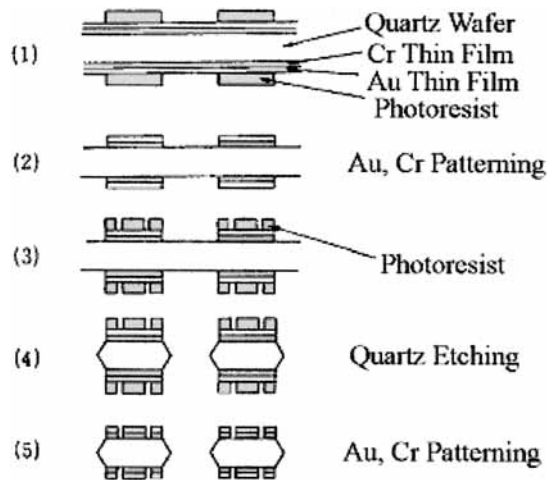


Fig. 2. Patterning procedures.

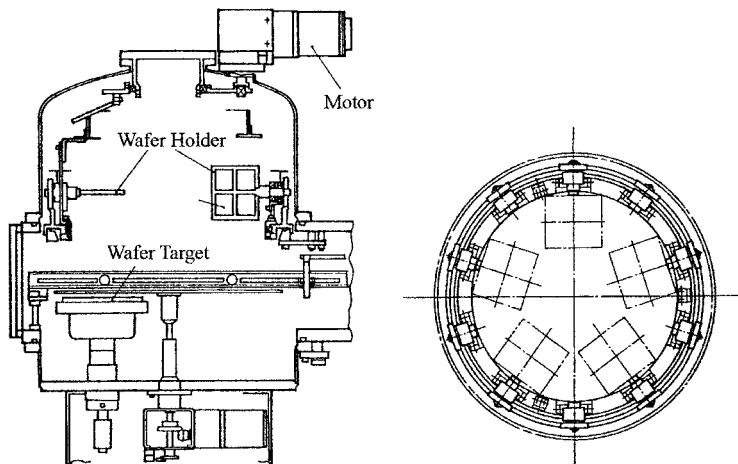


Fig. 3. Double-sided sputtering system.

its suitability for micromachining quartz. This equipment was developed to manufacture rectifiers and power transistors. It has been in use in this field since micromachining technology began being employed in the manufacture of quartz oscillators for electronic watches.

This equipment is a double-sided exposure unit that uses a projection method having a projection magnification of 1:1. It meets the requirement for double-sided printing of having the same optical system on its top and bottom parts. A dummy wafer is used to align the top and bottom photomask images with each other. The dummy wafer shifts the location of a single photomask image by a distance equivalent to the thickness of a wafer to

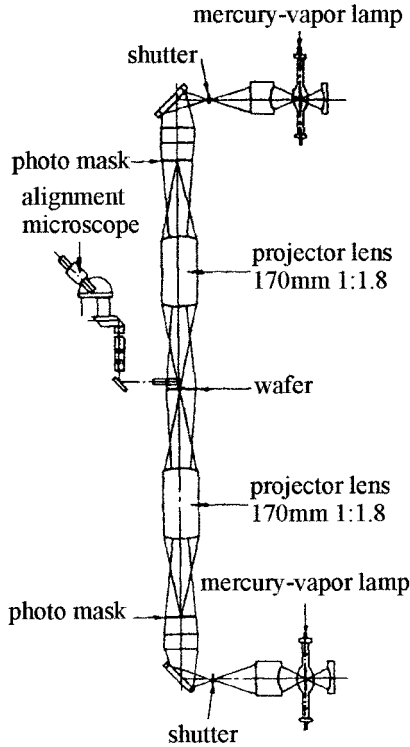


Fig. 4. Optical system of double-sided exposure equipment.

form the top and bottom photomask images on the same plane. The positions of the top and bottom photomasks are adjusted by observing these images through an alignment scope. As a result, a precisely located etching mask can be produced on both sides of a quartz wafer during the actual exposure.

Figure 5 explains the optical arrangement of this equipment and shows a diagram of the principle of a dummy wafer used to align the top and bottom images with each other.

When photolithography patterns are exposed, upper imaging light is focused on the top surface of a wafer and lower imaging light is focus on the bottom surface of the wafer. To align the patterns of both sides a dummy wafer is used. The dummy wafer is a type of glass, and we usually use quartz. The dummy wafer is a half mirror and its refractive index is n . Here, t is the thickness of the wafer, the thickness of the dummy wafer, T , is derived as follows; $T = t \cdot n / (n - 1)$. Therefore, when the dummy wafer is set up as shown in Fig. 5(1), we can observe both sides of the pattern over the top surface at once.

Figure 6 shows that the profile of the etching rate depends on the cut angles. The horizontal axis shows etching time and the vertical axis shows etched depth. Two cut angle sample etching rates are indicated. Black dots denote data for the plate perpendicular to z -axis and white dots denote data for the plate with a cut angle of -40.2 degrees relative to the y -axis. Both plots show that the etched depth is proportional to etching time.

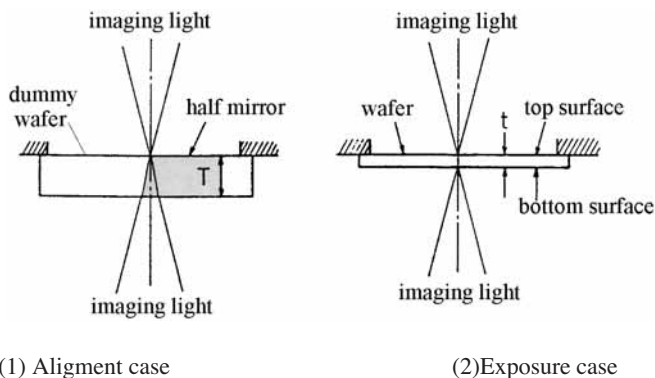


Fig. 5. Alignment of top and bottom images. (T : thickness of dummy wafer, t : thickness of wafer, n : refractive index of dummy wafer)

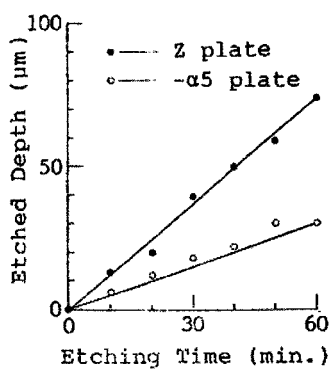


Fig. 6. Experimental results of quartz wafer etching rate.

The z -direction of the wafer was used to clarify the directions of minimum etching rate around the x -axis and y -axis. The designed striped mask patterns were formed on the z -wafer parallel to x -axis and y -axis. (Fig. 7) The directions of minimum etching rate were obtained by using the crystal faces produced by etching a z -directional α -quartz wafer plate with an attached striped metal mask under the above-mentioned condition. These photographs show cross sections of the etched z -directional wafer. The left side photographs shows a z -wafer whose striped pattern is parallel to the y -axis, and the right side photograph shows a z -wafer whose striped pattern is parallel to the x -axis.

Each graph in Fig. 8 shows the etching rate in the polar coordinate system. The left figure shows profiles parallel to the x -axis and parallel to the y -axis. The plotted points are experimental data. The experimental data points are fitted by a spline function.

Figure 9 shows three-dimensional representations of etching rates. This figure expresses the etching rates of the crystal faces in all directions of the quartz in polar

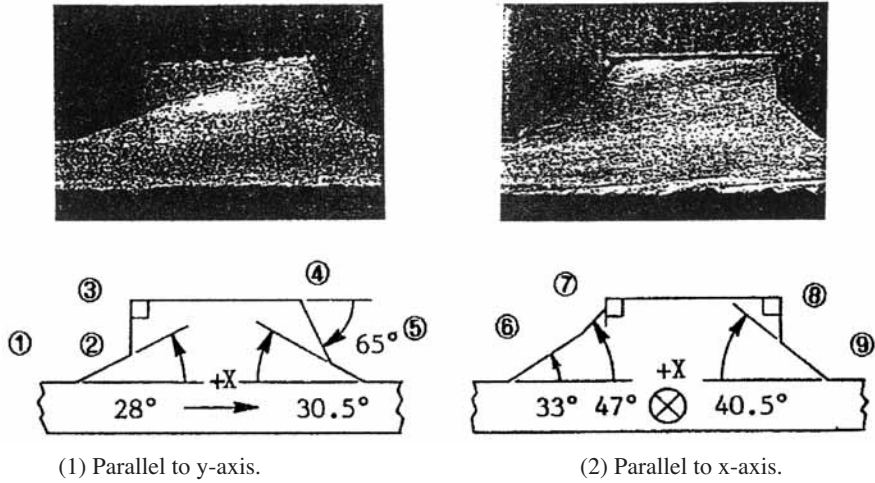


Fig. 7. Cross-sectional view of etched quartz wafer. Wafer: plane perpendicular to z-axis ($t = 0.5$ mm) Pattern: striped pattern parallel to x-axis and y-axis.

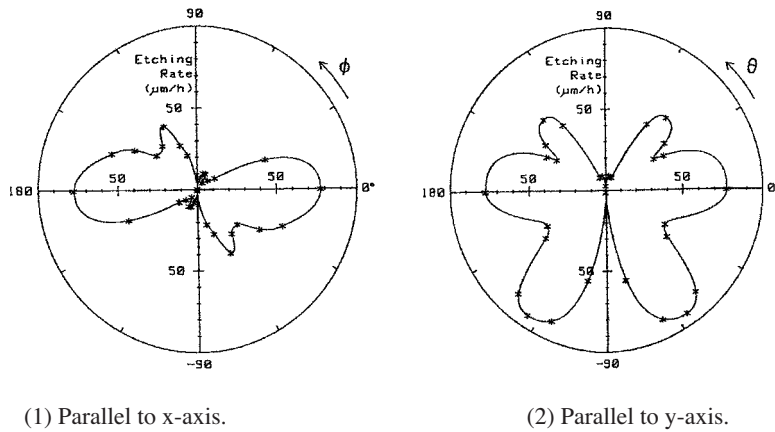


Fig. 8. Polar diagrams for normal etching rate of quartz wafer cut parallel to the x-axis and y-axis. ϕ : angle from z plate (along $\langle 100 \rangle$ zone axis) θ : angle from z plate (along $\langle 120 \rangle$ zone axis)

coordinates as denoted by different contrast, which have been calculated on the basis of experimental data shown in stereoscopic projection by the aforementioned procedure. The distance from the center of the coordinates to the surface of the stereoscopic projection indicates the magnitude of the etching rates and the direction represents the direction of the normal line of crystal faces. These results enable us to confirm that the data of etching rates we used are basically consistent with the recent results reported by Cheng *et al.*⁽¹⁾

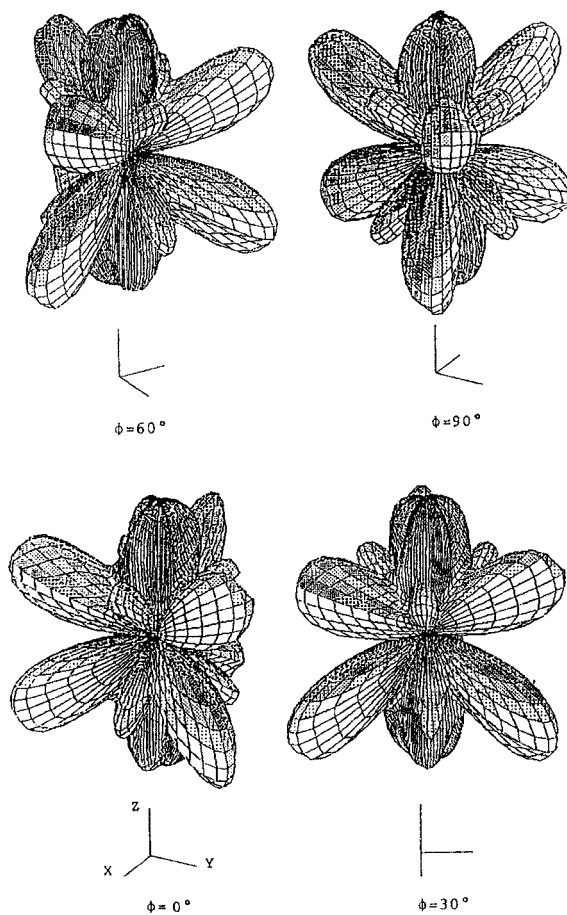


Fig. 9. Three-dimensional representation of etching rate.

4. Simulations

In this section we explain the simulation scheme for estimation of the cross section of alpha-quartz at any cut angle. The configuration of an alpha-quartz crystal face can be predicted by using the etching rate profile calculated from the experimental data. The lines perpendicular to the minimum etching rate directions surround the shape of the etched cross section. The simulation steps are as follows.

(1) Cut the etching rate profile on the plate from the 3D etching rate profile. (2) Determine the minimum inflection points from the etching rate profile. (3) Move the line perpendicular to the direction of etching at each rate. (4) The region enclosed above the etched lines and nonetching lines (metal mask lines) is the shape of the etched cross section.

By simulating the shape of micromachining components in this way, we can precisely estimate etching rates and the shape of the cross section in any directional cut of alpha-quartz wafers.

In this study, we determined the cross-sectional shape of a $-\alpha 5$ plate ($\phi = -40.2$, $\theta = 0$). This cut of plate is one of the most useful angles of wafer for quartz thermometers.

When the etching rates of crystal faces having the intersection line of the $-\alpha 5$ cut plate (0223 face) and y-cut plate (2110 face) as the zone axis are cut on the basis of the three-dimensional representation of the etching rate, a polar plot, as shown in Fig. 10, is obtained. In this plot, the etching rates of the alpha-quartz wafer are expressed by the length of the radius vector of the $\theta = 0^\circ$ direction, and the crystal face appearing on the cross section of a beam becomes a crystal face in the direction that takes a minimal etching rate in the same figure. Application of this technique to wafers having various cut angles allows prediction of the cross-sectional shape to be produced when micromachined.

Figure 11 shows the cross-sectional shape results of simulations and an experiment. Figures 11(a) to 11(c) show a continuous change in shape with etching time. Figure 11(d) shows a photograph of the cross-sectional shape obtained in the experiment. On the basis of these figures, we conclude that our estimated cross section almost agreed with the result of the experiment and that this technique resulted in successful prediction of the cross-sectional shapes.

5. Conclusions

(1) We confirmed that our proposed theory corresponded to the experimental data for etching rates of all directions of alpha-quartz. (2) Our estimation of the etched shape agreed with the experimental data. (3) The results of these simulations enable the development of three-dimensional computer-aided-design systems for the precision design of complex-shaped objects to be fabricated by anisotropic etching of alpha-quartz.

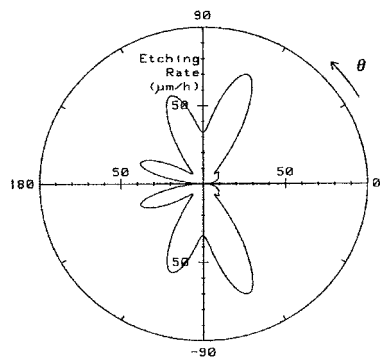


Fig. 10. Polar diagram of normal etching rate. θ : angle from $-\alpha 5$ plate (along $\langle 364 \rangle$ zone axis).

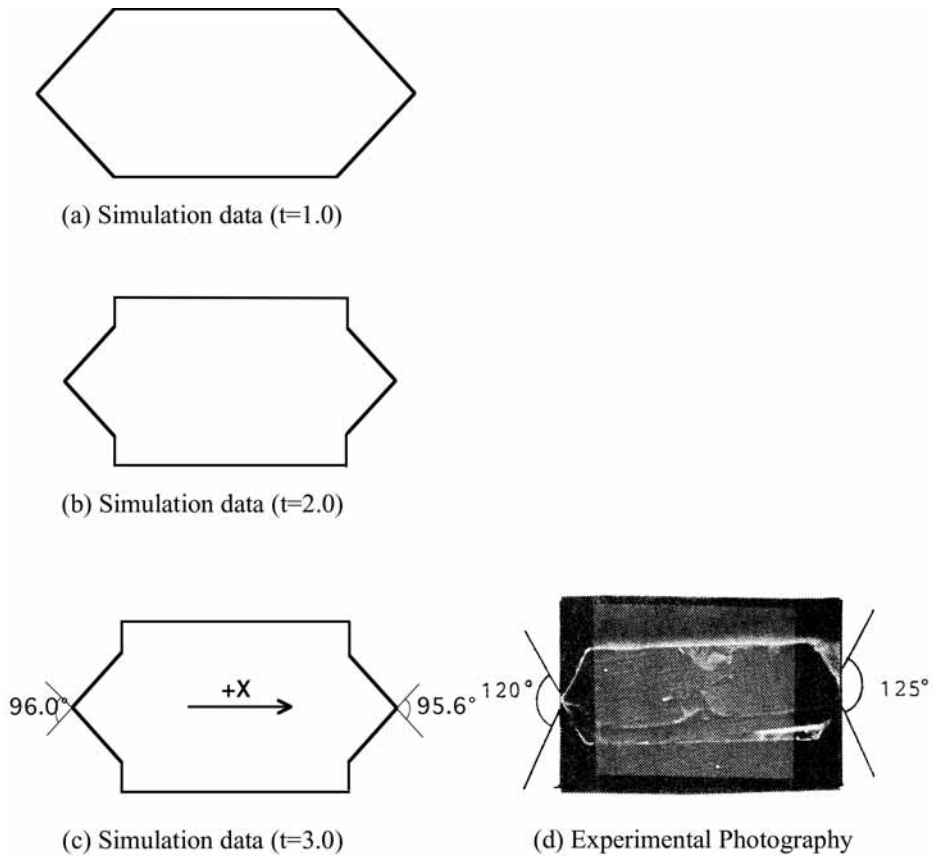


Fig. 11. Estimated shapes of cross-sectional view of quartz wafers.

References

- 1 D. Cheng, K. Sato, M. Shikida, A. Ono and K. Sato: Proc. 20th Sensor Symposium (2003) p. 379.
- 2 T. Ueda, F. Kohsaka, D. Yamazaki and T. Iino: Proc. 3rd Int. Conf. Solid-State Sensors and Actuators (TRANSDUCERS '85, 1985) p. 113.
- 3 T. Ueda, F. Kohsaka, T. Iino and D. Yamazaki: T-SICE **23** (1986) 1233. (in Japanese)
- 4 F. C. Frank: On the Kinematic Theory of Crystal Growth and Dissolution Processes, Growth and Perfection of Crystal (John Wiley, 1958) p. 411.
- 5 R. J. Jaccodine: J. App. Phys. **33** (1962) 2643.
- 6 B. W. Batterman and Hillocks: J. App. Phys. **28** (1957)1236.